ELSEVIER

Catalysis Today 48 (1999) 265–272

CATALYSIS TODAY

Mass transfer effects on hydroformylation catalyzed by a water soluble complex

A. Lekhal[a], R.V. Chaudhari[b], A.M. Wilhelm[a], H. Delmas[a,*]

[a]LGC, Laboratoire de génie chimique UMR 5503 CNRS, Toulouse, France
[b]NCL, National Chemical laboratory CSIR, Pune, India

Abstract

The rate of hydroformylation of 1-octene catalyzed by a water soluble catalyst is measured in mechanically agitated batch reactor at various stirrer speeds and organic phase holdups. The data have been analyzed by coupling reaction kinetics to a pseudo-homogeneous gas–liquid–liquid model based on Higbie's penetration theory which takes into account the presence of the dispersed organic phase. A rapid liquid–liquid mass transfer of the reactants is assumed leading to an equilibrium between the continuous and the dispersed phases. The predicted values of the rate are in good agreement with the experimental one. The depletion of the organic substrate in the continuous phase is found negligible. © 1999 Elsevier Science B.V. All rights reserved.

Keywords: Water soluble ligand; Aqueous phase catalysts; Gas–liquid mass transfer; Gas–liquid–liquid model; Multiphase reaction kinetics

1. Introduction

Hydroformylation of olefins is a well-known commercial process involving the reaction of an olefin with a mixture of CO and H_2 (syngas) in order to form linear and branched aldehydes. The reaction occurs in the presence of rhodium catalyst. The major problem associated with the use of rhodium catalyst has been its separation from the products. The recent modification by using a water soluble catalyst has been a major improvement in this direction [1]. The process uses an aqueous phase containing the catalyst and the water soluble ligand and the organic phase wherein the reactant and/or products are present. All the reactants should have high enough solubility in the aqueous phase, where the reaction is taking place. A theoretical thermodynamic investigation of liquid–liquid equilibria showed that for higher olefins like hexene and octene, the solubility in the aqueous phase is poor and provides a very low rate of reaction. The use of convenient cosolvents was proved to increase substantially the rate by improving the solubility of the organic substrate in the aqueous phase [2].

The kinetics of hydroformylation for two phase systems with water soluble catalysts has gained only poor attention. The kinetics of hydroformylation of 1-octene, in the presence of ethanol as cosolvent has been reported by Purwanto and Delmas [3]. A simple empirical rate model was developed. For the same reaction, Deshpande et al. [4] reported a semi empirical model and the following rate equation was proposed:

---

*Corresponding author.

PII: S0920-5861(98)00381-2

$$r = \frac{k\,C_A\,C_B\,C_C\,C_D}{(1 + K_a\,C_A)(1 + K_b\,C_B)^2}, \qquad (1)$$

where C_C is the catalyst concentration, C_A, C_B and C_D are the concentrations of hydrogen, carbon monoxide and olefin, respectively, within the catalytic aqueous phase. These kinetic studies have been developed avoiding any mass transfer limitations. In large scale reactions, gas–liquid mass transfer may be limiting.

The simultaneous absorption of two gases followed by simple or complex reaction kinetics is studied in gas–liquid systems [5–9]. However, there has been no attempt so far to analyze a case of simultaneous absorption of two gases which react with a liquid substrate in biphasic media.

The aim of this paper is to test a mass transfer model based on the penetration theory for the prediction of the rate of hydroformylation in heterogeneous liquid–liquid system under gas–liquid mass transfer limitations. It is known from previous work that for H_2 and CO the liquid–liquid mass transfer is not a limiting step [10]. We have also assumed that the olefin was in equilibrium between the two liquid phases. The influence of parameters such as stirrer speed and volume fraction of the organic phase has been investigated in a wide range.

2. Experimental

The precursor catalyst used is $[Rh(COD)Cl]_2$ which was purchased from Fluka, Switzerland. The water soluble ligand is TPPTS. It was used directly as a 30% (w/w) solution in water. Hydrogen and carbon monoxide are obtained from AGA, France. 1-octene was procured from Aldrich Chemical, whereas Rectapur ethanol was used from Rectapur (95% aqueous solution).

The experiments were carried out in 6×10^{-4} m^3 capacity autoclave (autoclave engineers) equipped with a gas inducing turbine with variable stirring speed up to 2500 rpm. The equipment was provided with automatic temperature control and pressure recording system. The temperature of the liquid in the reactor could be controlled within 1 K. A fast and accurate pressure transducer (±1 kPa) was used to measure the variation of the autoclave pressure. The transducer signal was transmitted to an acquisition card and recorded on-line by a PC. A schematic diagram of the apparatus is shown in Fig. 1.

In a typical procedure, a known volume of water is added to the required amounts of TPPTS, catalyst and ethanol (cosolvent). At higher temperatures, ethanol can undergo interactions with aldehydes to form acetals. To avoid the formation of acetals, the reactions were carried out at a pH of 10.

Finally, a mixture of octane and 1-octene is added to the aqueous phase in the requisite quantities. The content was heated to a desired temperature. After the thermal equilibrium was attained, the void space in the reactor was carefully flushed with a known quantity of H_2 and CO and pressurized to the selected level. The reaction was started by switching the stirrer on.

3. Theory

The reaction of hydroformylation occurring in the aqueous phase can be represented by:

$$\mathrm{A(g)} + \mathrm{B(g)} + \mathrm{D(l)} \underset{\text{catalyst}}{\rightarrow} \text{product} \qquad (2)$$

The following assumptions can be made:

- The gas-side mass transfer resistance is negligible.
- Henry's law is applicable.
- Direct gas/organic phase contact is not promoted.
- Isothermal conditions prevail.
- Semibatch mode of operation.
- Liquid–liquid equilibrium is assumed in all the reactants.

To ensure that the liquid–liquid mass transfer of 1-octene is not limiting, we can compare the maximum rate of the reaction to the maximum rate of 1-octene mass transfer. If we consider that the organic (dispersed) phase is present in the form of spherical droplets with a negligible slip velocity with respect to the continuous phase, we can estimate a liquid mass transfer coefficient k_{ll} by using $Sh=2$:

$$k_{ll} = \frac{2\,D_{OC}}{d_p}, \qquad (3)$$

where D_{oc} is the molecular diffusivity of 1-octene in the organic phase calculated by using Diaz equation [11] and d_p the droplet diameter which is estimated at 20 μm from separate experiments with laser granul-

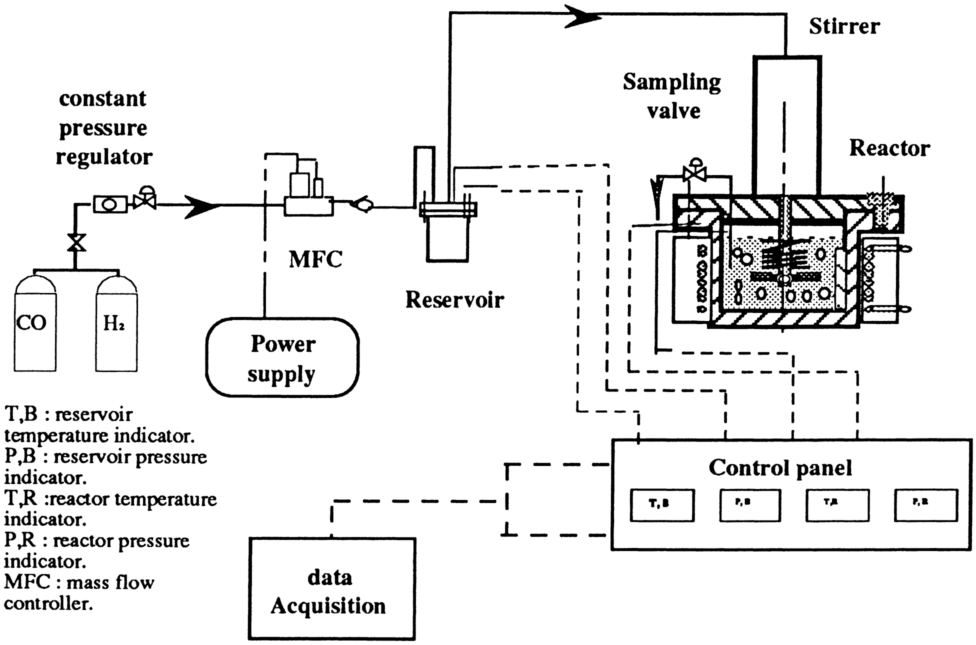

Fig. 1. Schematic of experimental set-up.

ometer. Furthermore, if it is assumed that no agglomeration of the dispersed phase occurs, the specific liquid–liquid interfacial area may be approximated by:

$$a_{\mathrm{ll}} = \frac{6\epsilon}{d_{\mathrm{p}}}, \tag{4}$$

and the liquid–liquid volumetric coefficient can be:

$$K_{\mathrm{OC}} = \frac{12\epsilon D_{\mathrm{OC}}}{d_{\mathrm{p}}^2}. \tag{5}$$

For ϵ=0.2, K_{oc} was found equal to 60 and the ratio of the rate to 3×10^{-4}. This low value proved that the liquid mass transfer of 1-octene is extremely rapid with respect to the rate of reaction and that a liquid–liquid equilibrium of the organic substrate may be assumed.

Eq. (1) is used in the present analysis for representing the true kinetics of the reaction. Uniform concentration of the catalyst is assumed in the aqueous phase, then Eq. (1) becomes:

$$r = \frac{k' C_{\mathrm{A}} C_{\mathrm{B}} C_{\mathrm{D}}}{(1 + K_{\mathrm{a}} C_{\mathrm{A}})(1 + K_{\mathrm{b}} C_{\mathrm{B}})^2}, \tag{6}$$

where $k'=kC_{\mathrm{C}}$.

The problem of simultaneous absorption of two gases A and B which react with an olefin D in an aqueous phase, may be represented by the following material balance equations, where C_i are the concentrations in the aqueous phase and x the distance from the gas–liquid interface:

$$(1-\epsilon)D_{\mathrm{A}} \frac{\partial^2 C_{\mathrm{A}}}{\partial x^2} = (1 - \epsilon + \epsilon m_{\mathrm{A}}) \frac{\partial C_{\mathrm{A}}}{\partial t} + (1-\epsilon) r_{\mathrm{A}}, \tag{7}$$

$$(1-\epsilon)D_{\mathrm{B}} \frac{\partial^2 C_{\mathrm{B}}}{\partial x^2} = (1 - \epsilon + \epsilon m_{\mathrm{B}}) \frac{\partial C_{\mathrm{B}}}{\partial t} + (1-\epsilon) r_{\mathrm{B}}, \tag{8}$$

$$(1-)D_{\mathrm{D}} \frac{\partial^2 C_{\mathrm{D}}}{\partial x^2} = (1 - \epsilon + \epsilon m_{\mathrm{D}}) \frac{\partial C_{\mathrm{D}}}{\partial t} + (1-\epsilon) r_{\mathrm{D}}, \tag{9}$$

with the initial and boundary conditions:

$$t = 0, \quad x > 0, \quad C_{\mathrm{A}} = C_{\mathrm{B}} = 0, \tag{10a}$$

$$t = 0, \quad x > 0, \quad C_{\mathrm{D}} = C_{\mathrm{D}} = 0, \tag{10b}$$

$$t > 0, \quad x = 0, \quad C_{\mathrm{A}} = C_{\mathrm{A}}^* \text{ and } C_{\mathrm{B}} = C_{\mathrm{B}}^*, \tag{10c}$$

$$t > 0, \quad x = 0, \quad \frac{\partial C_D}{\partial x} = 0, \tag{10d}$$

$$t = 0, \quad x = \infty, \quad \frac{\partial C_A}{\partial x} = \frac{\partial C_B}{\partial x} = \frac{\partial C_D}{\partial x} = 0. \tag{10e}$$

Eq. (10d) represents the non-volatility of the organic substrate at the gas–liquid interface (zero transport at the interface). The relative solubilities m_A, m_B and m_D, can be approximated by the ratio of the solubility of a reactant in the organic phase to that in the aqueous one. The symbols used in the set of equations (7)–(10) are defined in Section 6.

The set of Eqs. (7), (8) and (9) consists of parabolic partial differential equations (PDEs) which were solved numerically by the method of lines. The PDEs were converted to ordinary differential equations (ODEs) by discretization of the spatial derivatives, applying central difference formulas:

$$\left(\frac{\partial^2 C_A}{\partial x^2}\right)_{x_i} \approx \frac{C_{A_{i+1}} - 2C_{A_i} + C_{A_{i-1}}}{\Delta x^2} \tag{11}$$

Δx is the length of the grid size. We can define i as the point having the coordinate $i(\Delta x)$.

The system of ODEs obtained was solved with respect to time by the backward difference method (Gear's method) using the ODE-solver LSODAR.

From physical absorption, we have found that H_2 and CO were absorbed practically at the same rate. The specific rates of reactions are based on gases flux and defined from the penetration theory as

$$\varphi_B = \frac{1}{t_c}\int_0^{t_c} -D_B\left(\frac{\partial C_B}{\partial x}\right)_{x=0} dt, \tag{12}$$

where t_c is the contact time given by

$$t_c = \frac{4D_B}{\pi k_1^2}. \tag{13}$$

The diffusion coefficient D_B is estimated by using Diaz equation [11] and the mass transfer coefficient k_1 from Calderbank equation [9].

The first derivative is obtained by applying central difference formulas and it can be written as:

$$\left(\frac{\partial C_B}{\partial x}\right)_{x=0} \approx \frac{-3CB_0 + 4C_{B_1} - C_{B_2}}{2\Delta x}. \tag{14}$$

The integral in Eq. (12) was solved numerically using the trapezoidal rule. The rate of absorption is obtained by multipling φ_B by the gas–liquid interfacial area a which is deduced from the volumetric coefficient k_1a which has been determined by Lekhal et al. [10].

$$R_B = a\varphi_B. \tag{15}$$

4. Results and discussion

4.1. Determination of k_1a

First, we determined k_1a for CO in organic (octane+ octene)-aqueous (water+ethanol+TPPTS) emulsions.

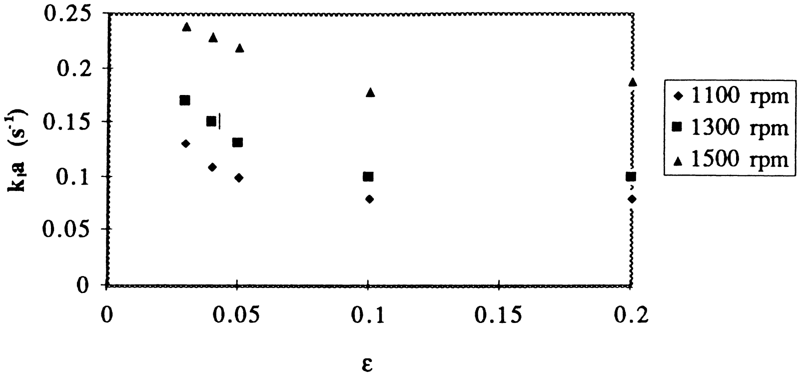

Fig. 2. Variation of k_1a for CO versus organic phase holdup for different stirrer speeds; P=1 Mpa, T=343 K.

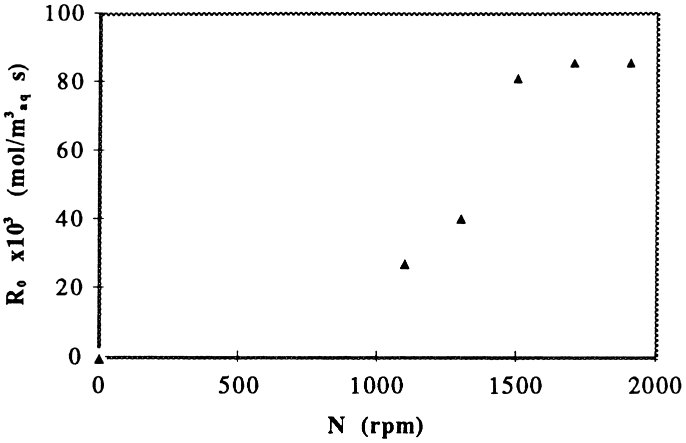

Fig. 3. Determination of the regime of absorption versus the stirrer speed.

As expected, an increase in the stirrer speed leads to an increase in k_1a. On the other hand, as mentioned by Lekhal et al. [10], k_1a decreases with the organic phase holdup ϵ beyond 3% (Fig. 2).

4.2. Determination of the regime of absorption

It was necessary to ensure that the data were obtained under mass transfer limitations. For this purpose, we have represented in Fig. 3, the variation of the reaction rate versus the stirrer speed at a fixed catalyst concentration. It appears clearly that above 1700 rpm, the rate of hydroformylation has reached a constant value which corresponds to the kinetic regime. Below this value, the rate of the reaction increases with the stirrer speed which is proving the reaction to occur under some gas–liquid mass transfer limitation.

4.3. Experimental results

The preliminary experiments proved that the material balance reactants/products is consistent (material balance >95%). The solubility of 1-octene in the aqueous phase is obtained by the UNIFAC approach, using PROPHY software [12].

The solubilities of H_2 and CO were measured in the reaction medium at the desired temperature (343 K) and pressure (1 MPa) by dynamic absorption [10]. To ensure stability of the catalytic complex, the molar ratio of rhodium to TPPTS is fixed at 1:8. The range of conditions investigated in this study is summarized in Table 1.

4.3.1. Effect of stirrer speed

Fig. 4 (as Fig. 3) shows that the reaction rate increases with an increase in stirrer speed. At lower stirrer speed, the substrate concentrations within the catalytic phase tend to be negligible, indicating diffusion control. With a further increase in agitation, the substrate concentrations reached the equilibrium values, thus approaching the kinetic regime and the rate tends to be independent of stirrer speed. The effect of agitation is more important at high values of organic phase holdups (beyond 5%).

Selectivity on linear aldehyde is not affected by mass transfer limitations and was always close to 75%.

Table 1
Range of experimental conditions

Catalyst $[Rh(COD)Cl]_2$	1.52 mol m^{-3}
Partial pressure of CO	1 MPa
Partial pressure of H_2	1 MPa
Olefin concentration	26.6–30 mol m^{-3}
P/Rh ratio	8 mol/mol
Temperature	343 K
Cosolvent	Ethanol
Holdup ratio organic/total	0.03–0.2 (v/v)
Reaction volume	3×10^{-4} m^3
Agitation speed	1100–1500 rpm

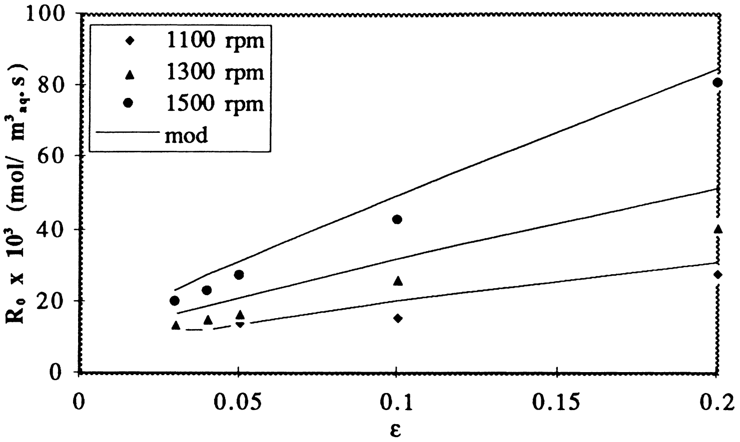

Fig. 4. Variation of the rate of hydroformylation versus organic phase holdup at various stirrer speeds; T=343 K, P=2 Mpa.

4.3.2. *Effect of organic phase holdup*

Experimental data clearly show that the rate of hydroformylation increases substantially with the organic phase holdups. Even though k_1a decreases with ϵ, the essential action of the organic dispersed phase is to interact with the diffusing solute near the interface in such a way so as to remove it from the vicinity of the interface by facilitating its transport into the bulk of the continuous phase where the gas is sparingly soluble. On the other hand, the solubilities of 1-octene (Fig. 5), H_2 and CO in the aqueous continuous phase increase with ϵ, which also increases the local rate of the reaction. The net effect of ϵ on the rate of the reaction will depend on the relative importance of all these competing phenomena.

The influence of ϵ is more pronounced at 1500 rpm because the mobility of the dispersed phase may be more important at this stirrer speed.

4.4. *Theoretical results*

Typical profiles of concentrations of dissolved gases and 1-octene within the aqueous phase are presented in Fig. 6(a) and (b). As expected the concentration of the dissolved gas decreases from the interface to the bulk of the liquid, while the concen-

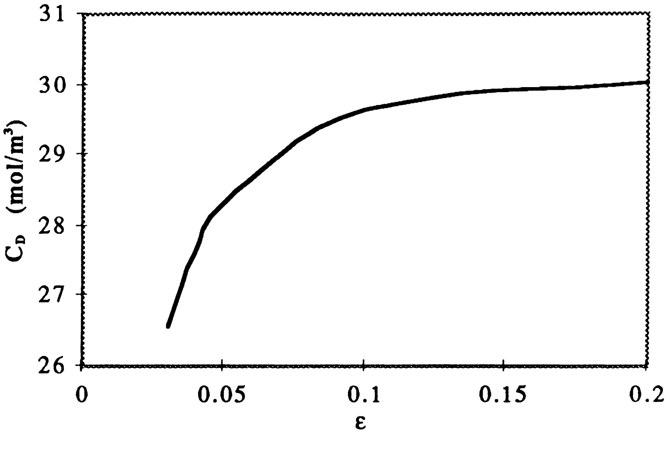

Fig. 5. Variation of the solubility of 1-octene in the aqueous phase versus organic phase holdup; T=343 K, P=2 Mpa.

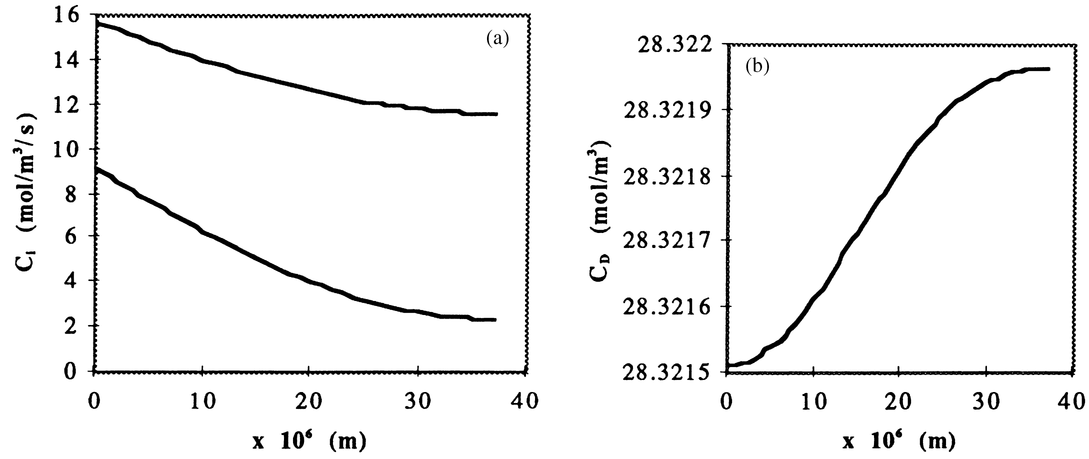

Fig. 6. (a) Typical profile of dissolved gases in the continuous phase. (b) Typical profile of 1-octene in the continuous phase.

tration of 1-octene increases slightly: the difference in concentration between the interface and the bulk is less than 0.002%, also the profile can be considered as flat. The 1-octene consumed by the reaction in the continuous phase is rapidly substitued by fresh substrate from the organic phase. This result confirms the fact that the mass transfer of 1-octene to the aqueous phase is extremely rapid and not limiting.

In this case the proposed model can be simplified by dropping Eq. (6) and the concentration of 1-octene may be considered as in excess in the continuous aqueous phase.

The rate of hydroformylation reaction is predicted by model equations (7)–(10). As can be seen from Fig. 4, the model describes reasonably the experimental values especially at low stirrer speed. The difference between the predicted and observed values never exceeds 20%.

5. Conclusion

The rate of reaction of hydroformylation of 1-octene in biphasic media has been conveniently analyzed by a model coupling true kinetics of the reaction and experimental gas–liquid mass transfer data obtained previously. The effects of the main parameters, stirrer speed and organic phase holdups, have been discussed. This model without any fitting parameter does not need to know the regime of absorption.

The convenient agreement with the experimental reaction runs proved the main hypothesis, i.e. liquid–liquid equilibria to be valid in these reaction conditions and gas–liquid mass transfer of CO and H_2 to be the only limitation.

6. Nomenclature

a	specific gas–liquid interfacial area (m^2/m^3 tot.)
a_{ll}	liquid–liquid interfacial area (m^2/m^3 tot.)
C_i	concentration of gas in the continuous phase (mol/m^3 cont.)
C_i^*	concentration of gas at the gas–liquid interface (mol/m^3 cont.)
C_C	concentration of catalyst in the continuous phase (mol/m^3 cont.)
C_D	concentration of 1-octene in the continuous phase (mol/m^3 cont.)
C_{D0}	initial concentration of 1-octene in the continuous phase (mol/m^3 cont.)
D_i	diffusivity of the dissolved gas in the continuous phase (m^2/s)
D_D	diffusivity of 1-octene in the continuous phase (m^2/s)
d_p	droplet diameter of dispersed phase (m)
D_{oc}	diffusivity of 1-octene in the organic phase (m^2/s)
k, k', K_a and K_b	kinetic constants defined in Eqs. (1) and (6)

k_1	gas–liquid mass transfer coefficient (liquid side) (m/s)
k_{ll}	liquid–liquid mass transfer coefficient (continuous side) (m/s)
K_{oc}	transport coefficient of 1-octene in continuous phase (l/s)
m_i	distribution coefficient of gas between dispersed and continuous phase (mol/m^3 disp.)/(mol/m^3 cont.)
m_D	distribution coefficient of 1-octene between dispersed and continuous phase (mol/m^3 disp.)/(mol/m^3 cont.)
r	rate of reaction (mol/m^3 cont.)
R_B	rate of reaction under mass transfer limitations (mol/m^3 cont.)
t	microscale time (s)
t_c	contact time (s)
x	distance from gas–liquid interface (m)

Greek symbols

ϵ	volume fraction of the dispersed phase (m^3 disp./m^3 tot.)
φ	specific rate of CO (mol/m^2/s)

Indices

A,B	H_2 and CO respectively
D	1-octene

Acknowledgements

The authors wish to thank IFCPAR (Indo-French Center for the Promotion of Advanced Research) for financial support.

References

[1] E.G. Kuntz, CHEMTECH 17 (1987) 570.

[2] I. Hablot, J. Jenck, G. Casamatta, H. Delmas, Chem. Eng. Sci. 47 (1992) 2689.

[3] O. Purwanto, H. Delmas, Catal. Today 24 (1995) 135.

[4] R.M. Desphande, O. Purwanto, H. Delmas, R.V. Chaudhari, Ind. Eng. Chem. Res. 35 (1996) 3927.

[5] G.H. Roper, T.F. Hatch, R.L. Pigford, Ind. Eng. Chem. Fundls. 1 (1962) 144.

[6] P.A. Ramachandran, Chem. Eng. Sci. 26 (1971) 349.

[7] R.V. Chaudhari, L.K. Doraiswamy, Chem. Eng. Sci. 29 (1974) 675.

[8] R. Cornelisse, A.A.C.M. Beenackers, F.P.H. Van Beckum, W.P.M. Van Swaaij, Chem. Eng. Sci. 35 (1980) 1245.

[9] A. Battacharya, R.V. Chaudhari, Ind. Eng. Chem. Res. 26 (1987) 1168.

[10] A. Lekhal, R.V. Chaudhari, A.M. Wilhelm, H. Delmas, Chem. Eng. Sci. 52 (1997) 4069.

[11] M. Diaz, A. Vega, J. Coca, Chem. Eng. Commun. 52 (1987) 271.

[12] X. Joulia, B. Koehret, J.M. Le Lann, F. Lambolez, Sere Peyrigain, Prosim, Toulouse, France, 1987.